Research Square

Preprints are preliminary reports that have not undergone peer review.
They should not be considered conclusive, used to inform clinical practice,
or referenced by the media as validated information.

Structural decoupling index–based characterization of hierarchical brain structure–function coupling alterations and their clinical and molecular associations in migraine: a cross-sectional study

Zhi Guo
Beijing Tiantan Hospital, Capital Medical University
Zhonghua Xiong
Beijing Tiantan Hospital, Capital Medical University
Yanliang Mei
Beijing Tiantan Hospital, Capital Medical University
Di Zhang
School of Artificial Intelligence, Beijing University of Posts and Telecommunications
Dong Qiu
Beijing Tiantan Hospital, Capital Medical University
Cunxin Lin
The First Affiliated Hospital of Zhengzhou University
Yongxiang Zhang
Beijing Tiantan Hospital, Capital Medical University
Geyu Liu
Beijing Tiantan Hospital, Capital Medical University
Tianshuang Gao
Beijing Tiantan Hospital, Capital Medical University
Yaqing Zhang
Beijing Tiantan Hospital, Capital Medical University
Xueying Yu
Beijing Tiantan Hospital, Capital Medical University
Hefei Tang
Beijing Tiantan Hospital, Capital Medical University
Xin Liu
Beijing Tiantan Hospital, Capital Medical University
Yong Liu
School of Artificial Intelligence, Beijing University of Posts and Telecommunications
Yonggang Wang
w100yg@gmail.com

Beijing Tiantan Hospital, Capital Medical University

Research Article

Keywords: migraine, structural decoupling index, structure–function coupling, graph signal processing, diffusion MRI, resting-state functional MRI

Posted Date: August 6th, 2026

DOI: https://doi.org/10.21203/rs.3.rs-10527929/v1

License: This work is licensed under a Creative Commons Attribution 4.0 International License. Read Full License

Additional Declarations: No competing interests reported.

Version of Record: A version of this preprint was published at The Journal of Headache and Pain on September 30th, 2026. See the published version at https://doi.org/10.1186/s10194-026-02525-6.

Abstract

BACKGROUND

Migraine is increasingly recognized as a network disorder involving distributed structural and functional brain alterations. However, regional changes in the relationship between resting-state activity and white-matter organization remain unclear. We used the structural decoupling index (SDI), a graph signal processing measure of structure–function alignment, to characterize regional coupling alterations in migraine.

METHODS

After quality control, 108 participants (41 with episodic migraine [EM], 31 with chronic migraine [CM], and 36 healthy controls [HCs]) underwent resting-state functional, diffusion, and T1-weighted MRI. Regional SDI was computed for 246 Brainnetome regions using individual RD-weighted structural graphs. Group differences were tested by age- and sex-adjusted ANCOVA with Benjamini–Hochberg FDR correction. Partial Spearman correlations examined associations between clinical measures and SDI in regions differing between EM and CM, adjusting for age, sex, and migraine subtype. Exploratory classification used class-weighted linear SVMs with repeated nested fivefold cross-validation. PLS regression related the unthresholded migraine–HC SDI t-map to Allen Human Brain Atlas gene-expression data, followed by enrichment analysis of genes with positive and negative PLS1 weights.

RESULTS

Compared with HCs, patients with migraine had lower SDI in the left superior frontal gyrus and higher SDI in the right inferior temporal gyrus. Three-group analyses additionally identified differences in the left lateral occipital cortex, where CM showed lower SDI than EM; lower values were associated with more monthly migraine days. Regional SDI features showed preliminary discrimination, strongest for CM versus HCs (AUC = 0.866). Positive PLS1-weighted genes were enriched in chromatin regulation, transcriptional control, and RNA metabolism, whereas negative-weighted genes were enriched in mitochondrial energy metabolism, oxidative phosphorylation, ribosome-associated quality control, and calcium signaling.

CONCLUSIONS

This first application of SDI to migraine revealed bidirectional hierarchical structure–function disruptions across prefrontal, temporal, and occipital regions. Lower lateral occipital SDI was associated with more monthly migraine days, while regional SDI features showed preliminary within-sample discrimination, strongest for CM versus HCs (AUC = 0.866). Transcriptomic enrichment implicated chromatin regulation and mitochondrial energy metabolism. SDI may provide a useful framework for characterizing hierarchical brain network dysfunction in migraine.

Introduction

Migraine is a highly prevalent and disabling neurological disorder characterized by recurrent attacks of moderate to severe headache, frequently accompanied by sensory hypersensitivity, cognitive dysfunction, and emotional disturbances[1–3]. Accumulating neuroimaging evidence suggests that migraine is not attributable to dysfunction within a single brain region, but rather represents a network-level disorder involving distributed structural and functional alterations across multiple cortical and subcortical circuits[4, 5]. Diffusion MRI (dMRI) studies have revealed widespread white matter microstructural abnormalities in migraine[6], particularly in frontal, temporal, and subcortical regions[7]. Notably, some studies have reported increased radial diffusivity in frontal white matter and in chronic relative to episodic migraine, suggesting alterations in diffusion perpendicular to the principal fiber orientation that may reflect myelin-related changes, among other microstructural processes[8, 9]. Resting-state functional MRI (rs-fMRI) studies have identified aberrant functional connectivity within pain-processing, executive control, and limbic networks[10, 11]. Graph-theoretical analyses have further demonstrated disrupted topological organization of the

structural connectome in chronic migraine, including reduced global and local efficiency and altered nodal properties in prefrontal and temporal regions[12]. Collectively, these findings suggest that the interaction between brain structure and function may be critically altered in migraine.

The human brain is organized as a hierarchical network[13] in which anatomical white matter pathways constrain and shape functional dynamics[14, 15]. The extent to which functional activity is constrained by the underlying structural scaffold, commonly referred to as structure–function coupling (SFC), varies systematically across the cortical hierarchy. Primary sensorimotor regions typically exhibit strong coupling, whereas transmodal association cortices show relative decoupling, a gradient organization thought to support functional flexibility and diverse cognitive repertoires[16, 17]. Aberrant SFC has been implicated in various neurological and psychiatric disorders and may provide a more sensitive marker of disease-related symptoms and cognitive impairment than structural or functional measures alone[17]. In migraine, a previous connectomics study reported globally reduced SFC, particularly involving rich-club and feeder connections, with associations with headache duration[18]. However, conventional correlational approaches primarily capture the linear correspondence between structural and functional connectivity strength, and may not fully characterize the hierarchical organization of brain function, in which functional activity decouples from structure in a regionally specific manner along the sensory-to-transmodal gradient[16].

To overcome this limitation, Preti and Van De Ville introduced the structural decoupling index (SDI), a graph signal processing-based framework that decomposes functional activity into components coupled to and decoupled from the underlying structural connectome harmonics, thereby quantifying the hierarchical dependency of regional brain function on structural architecture[16]. SDI has since been applied to characterize hierarchical structure–function disruption in Alzheimer's disease, revealing regionally specific decoupling patterns associated with cognitive decline and molecular pathways[19]. However, no study has yet applied the SDI framework to investigate the hierarchical organization of structure–function relationships in migraine. Whether and how the brain's macroscale structure–function hierarchy is disrupted in this disorder therefore remains unknown.

Here, we combined rs-fMRI and dMRI data from patients with migraine and healthy controls to compute regional SDI and systematically map hierarchical structure–function dysregulation in migraine. We further examined the clinical relevance of SDI alterations by assessing their associations with headache-related clinical measures, affective symptoms, and sleep quality, and explored potential molecular mechanisms using spatial gene expression enrichment analysis. We hypothesized that migraine would be characterized by regionally heterogeneous and bidirectional SDI alterations, reflecting dysregulation along the unimodal–transmodal hierarchy, and that these alterations would be associated with clinical symptom burden and molecular pathways related to neurotransmitter regulation, metabolism, and neurodevelopment.

Methods

Participants

This was a cross-sectional observational study. A total of 130 participants were enrolled, comprising 48 patients with episodic migraine (EM), 37 patients with chronic migraine (CM), and 45 healthy controls (HCs), were consecutively recruited from the Headache Center, Department of Neurology, Beijing Tiantan Hospital, Capital Medical University between September 2024 and July 2025. Patients with migraine were prospectively recruited and diagnosed according to the International Classification of Headache Disorders, 3rd edition (ICHD-3)[20]. All diagnoses were confirmed by experienced headache specialists. The inclusion criteria for migraine patients were as follows: diagnosis of migraine without aura; age between 14 and 65 years; history of migraine for more than one year; right-handedness; and eligibility for magnetic resonance imaging (MRI).The exclusion criteria for migraine patients included: coexistence of other primary headache disorders or chronic pain conditions; claustrophobia or other contraindications to MRI; inadequate MRI image quality; history of traumatic brain injury or neurological disorders; current or past major psychiatric disorders; cardiovascular or other major systemic diseases; use of preventive medications for more than three consecutive months prior to enrollment; and use of acute analgesics within two days before the MRI scan.Healthy controls were recruited if they were matched to the migraine group with respect to age and sex, were right-handed, eligible for MRI scanning, and no structural abnormalities on cranial imaging. Additional inclusion criteria for healthy controls included no history of neurological, psychiatric, or major systemic diseases. Exclusion criteria for healthy controls included pregnancy or

lactation, contraindications to MRI, and insufficient MRI data quality. All healthy controls underwent MRI scanning, whereas migraine patients completed both MRI scanning and clinical assessments during the interictal period.

Demographic and clinical characteristics and neuropsychological assessments

Demographic information, including age, sex, and body mass index (BMI), was systematically collected from all participants. For patients with migraine, clinical characteristics and clinical assessments scores were additionally recorded, including headache attack duration, pain intensity assessed using the Visual Analogue Scale (VAS)[21], monthly migraine days (MMD), the Migraine Disability Assessment (MIDAS)[22], the Headache Impact Test-6 (HIT-6)[23], the Generalized Anxiety Disorder-7 (GAD-7)[24], the Patient Health Questionnaire-9 (PHQ-9)[25], and the Pittsburgh Sleep Quality Index (PSQI)[26]. Global cognitive function was evaluated using the Mini-Mental State Examination (MMSE)[27] and the Montreal Cognitive Assessment (MoCA)[28]. Higher scores on the VAS, MIDAS, HIT-6, GAD-7, PHQ-9, and PSQI indicated greater pain intensity, disability, headache impact, psychological symptom severity, or poorer sleep quality, whereas higher MMSE and MoCA scores indicated better cognitive function.

MRI acquisition

All participants underwent brain MRI on a 3.0 T scanner using a 64-channel head/neck coil (MAGNETOM Prisma, Siemens Healthineers, Erlangen, Germany). During MRI acquisition, participants were instructed to remain still; during resting-state functional MRI, they were additionally instructed to keep their eyes closed.High-resolution T1-weighted structural images were acquired using a three-dimensional magnetization-prepared rapid gradient-echo sequence (3D MPRAGE) with the following parameters: echo time (TE) = 2.98 ms, repetition time (TR) = 2530 ms, inversion time (TI) = 935 ms, flip angle = 8°, isotropic voxel size = 1.0 × 1.0 × 1.0 mm^3, and generalized autocalibrating partial parallel acquisition (GRAPPA) parallel imaging with an acceleration factor of 2.Diffusion MRI data were acquired using a spin-echo echo-planar imaging diffusion sequence with TE = 69 ms, TR = 3500 ms, slice thickness = 2.0 mm, and a multiband acceleration factor of 3. To enable correction of susceptibility-induced distortions, an additional short b = 0 acquisition with the opposite phase-encoding direction was obtained. Specifically, the diffusion-weighted images were acquired with posterior-to-anterior phase encoding, and the additional b = 0 images were acquired with anterior-to-posterior phase encoding.Resting-state functional MRI data were acquired using a multiband gradient-echo echo-planar imaging blood oxygen level dependent (BOLD) sequence with TE = 30 ms, TR = 1000 ms, flip angle = 78°, slice thickness = 2.4 mm, and a multiband acceleration factor of 5.

MRI data processing and analysis

Diffusion MRI data were preprocessed using an MRtrix3-based[29] (https://www.mrtrix.org/) pipeline incorporating FSL[30] (https://fsl.fmrib.ox.ac.uk/), ANTs[31], and FreeSurfer[32](https://surfer.nmr.mgh.harvard.edu/). Preprocessing included denoising, Gibbs-ringing removal, correction for susceptibility-induced distortions, eddy-current–induced distortions and head motion, and bias-field correction. T1-weighted images were skull-stripped, nonlinearly registered to the MNI152 1-mm template, and subsequently resampled to 2-mm isotropic resolution. The mean b0 image derived from the preprocessed dMRI data was then registered to the normalized T1-weighted image, and the resulting transformations were applied to warp the dMRI data into MNI152 2-mm space. A five-tissue-type image and a white-matter mask were generated from the normalized T1-weighted image. Fiber orientation distributions were estimated using constrained spherical deconvolution, followed by whole-brain tractography using the white-matter mask for both seeding and tracking. An initial tractogram containing 2,000,000 streamlines was generated and subsequently filtered using spherical-deconvolution informed filtering of tractograms (SIFT) to retain 200,000 streamlines. A diffusion tensor model was fitted to generate radial diffusivity (RD) maps. The mean RD value along each streamline was calculated, and an RD-weighted, symmetric 246 × 246 structural connectivity matrix was constructed using the Brainnetome Atlas. Each edge represented the mean of the streamline-wise RD values across all streamlines connecting the corresponding pair of brain regions.

Resting-state functional MRI (rs-fMRI) data were preprocessed using the CONN toolbox (version 22a; https://web.conn-toolbox.org/) implemented in SPM12 (https://www.fil.ion.ucl.ac.uk/spm/software/spm12/). The first 10 volumes were discarded to allow for signal stabilization and participant adaptation. Preprocessing was performed using the default CONN indirect normalization pipeline in Montreal Neurological Institute (MNI) space. Slice-timing correction was omitted because of the short repetition time (TR = 1000 ms) and simultaneous multislice acquisition with a multiband acceleration factor of 5. The pipeline included functional realignment and unwarping, identification of outlier volumes, coregistration of the functional and T1-weighted images, tissue segmentation and spatial normalization to MNI space, resampling of the functional images to 2 × 2 × 2 mm³, and spatial smoothing using a Gaussian kernel with a 4-mm full width at half maximum. Participants exhibiting excessive head motion, defined as translation greater than 3 mm in any direction or rotation greater than 3°, were excluded. Denoising included linear detrending and regression of white-matter and cerebrospinal-fluid signals, a Friston-24–style expansion of the realignment parameters, and scrubbing regressors. Global signal regression was not performed. Temporal band-pass filtering was applied at 0.01–0.10 Hz. For region-of-interest–based analysis, the Brainnetome Atlas comprising 246 regions was applied to the denoised four-dimensional functional data, and the mean BOLD signal was extracted from each region. Each regional time series was demeaned across time, yielding a 246 × T matrix for each participant, where T denotes the number of retained time points.

Structure–function coupling

To quantify the coupling between structural connectivity and regional resting-state BOLD activity, SDI were calculated for each participant using a graph signal processing framework, following the method proposed by Preti and Van De Ville[16]. The individual RD-weighted structural connectivity matrix W was symmetrically normalized, and the normalized graph Laplacian was constructed as

$$L = I - D^{-1/2} W D^{-1/2},$$

where D denotes the diagonal degree matrix. Eigendecomposition of the Laplacian,

$$LU = U\Lambda\,,$$

yielded participant-specific structural connectome harmonics, with low- and high-frequency harmonics representing spatial patterns that were more strongly coupled to and decoupled from the structural network, respectively.

The regional BOLD time series were z-standardized across time and projected onto the structural harmonics. A participant-specific cutoff was defined as the frequency at which the cumulative spectral energy first reached 50% of the total energy following Preti et al[16]. The BOLD signals were subsequently decomposed into structurally coupled and decoupled components using ideal low- and high-pass graph spectral filters:

$$s_t^C = U_{\text{low}} U_{\text{low}}^T s_t,\; s_t^D = U_{\text{high}} U_{\text{high}}^T s_t,$$

The SDI of each brain region was calculated as the ratio of the euclidean norm of the decoupled and coupled signals across time:

$SDI_i = \frac{\| s_i^D \|_2}{\| s_i^C \|_2}$ SDI greater than 1 indicated a predominance of the structurally decoupled component, whereas an SDI below 1 indicated stronger coupling between regional BOLD activity and the RD-weighted structural network[33].

Difference analysis for SDI between migraine and HC

To assess group differences in regional SDI, region-wise analysis of covariance (ANCOVA) was performed separately for each of the 246 brain regions, with SDI as the dependent variable, group as the main factor, and age and sex as covariates. Two complementary analyses were conducted. First, EM and CM were combined into a single migraine group and compared with HC. Second, an overall three-group comparison among HC, EM, and CM was performed, followed by pairwise contrasts of EM versus HC, CM versus HC, and EM versus CM. Overall group effects were evaluated using partial F-tests. In the two-group analysis, BH-FDR correction was applied across the 246 regions to the HC–migraine group effect. In the three-group analysis, BH-FDR correction was applied separately across the 246 regions to the overall group effect and to each pairwise contrast. Statistical

significance was defined as $q_{\mathrm{FDR}} < 0.05$. Effect sizes for the overall group effects were quantified using partial eta-squared $\left(\eta_p^2\right)$, while covariate-adjusted group differences and their 95% CIs were reported for pairwise contrasts.

Associations between SDI alterations and clinical measures

To investigate the clinical relevance of SDI alterations, post hoc partial Spearman correlation analyses were performed in patients with migraine. SDI values were extracted from regions showing significant differences between the EM and CM groups after FDR correction in the preceding ANCOVA. HCs were not included because the clinical variables were migraine-specific and were not comprehensively assessed in this group. The clinical measures included headache attack duration, VAS, monthly migraine days, MIDAS, HIT-6, GAD-7, PHQ-9, PSQI, MMSE, and MoCA. Age, sex, and migraine subtype (EM or CM) were included as covariates. P-values were adjusted using the BH-FDR procedure across all region-by-clinical-variable tests within each SDI metric, with $q_{\mathrm{FDR}} < 0.05$considered statistically significant.

SVM classification and ROC analysis

To evaluate the discriminative ability of SDI alterations, a class-weighted linear support vector machine (SVM) was constructed using SDI values from regions showing significant group differences. Three pairwise classifications were performed: CM versus EM, CM versus HC, and EM versus HC. Model performance was assessed using repeated nested fivefold cross-validation with 30 repetitions. Age and sex effects were removed within each training fold, and the SVM cost parameter was selected by inner fivefold cross-validation. receiver operating characteristic (ROC) curves were generated from mean out-of-fold decision scores, and area under the curve (AUC) values with 95% confidence intervals (CIs) were estimated using 2,000 stratified bootstrap resamples.

Associations between gene expression and SDI alterations

To investigate the molecular mechanisms underlying SDI alterations in migraine, regional gene expression data from the Allen Human Brain Atlas[34] (http://human.brain-map.org/) were mapped to the Brainnetome Atlas using the Abagen toolbox[35] (https://abagen.readthedocs.io/en/stable/). Regions with invalid or missing expression data and genes with incomplete or invariant expression across the retained regions were excluded. PLS regression was performed using the regional gene expression matrix as predictors and the unthresholded, signed t-map of the migraine–HC difference in SDI as the response variable. Ten latent components were estimated using the SIMPLS algorithm after mean-centering both matrices. The significance of each PLS component was assessed using 5,000 ordinary row-wise permutations of the t-map, and the stability of gene weights was evaluated using 5,000 bootstrap resamples. The direction of PLS1 was oriented so that positive regional scores corresponded to higher signed t-values. Genes were ranked according to their signed PLS1 bootstrap ratios, and the top 1,000 positively and negatively weighted genes were analyzed separately using Metascape[36] (https://metascape.org/gp/index.html#/main/step1), with FDR $q < 0.05$ considered significant.

Results

Demographics and clinical characteristics

Among the 130 initially enrolled participants, 22 were excluded because of incomplete dMRI or rs-fMRI data, poor dMRI image quality, or excessive head motion. The final analysis included 108 participants: 36 HCs, 41 patients with EM, and 31 patients with CM (Fig. 1).

No significant differences were observed among the three groups in age, BMI, or sex distribution. However, when EM and CM were combined, the migraine group had a higher proportion of females than the HC group ($P = 0.030$). CM patients had higher VAS scores than EM patients [9 (8, 10) vs. 8 (7, 9), $P = 0.026$], whereas no significant differences were observed in headache attack duration, MIDAS, HIT-6, GAD-7, PHQ-9, or PSQI scores. MMSE and MoCA scores differed significantly among the three groups, and both were lower in the combined migraine group than in HCs (Table 1).

Table 1 Demographic and clinical characteristics of HC, EM, CM, and the combined migraine group

	Descriptive statistics				*P* value	
Variable	HC(n = 36)	EM (n = 41)	CM (n = 31)	Migraine(n = 72)	P_1	P_2
Age, years	32.22 ± 9.22	31.73 ± 11.81	37.58 ± 13.54	34.25 ± 12.83	0.129[a]	0.349[a]
BMI, kg/m²	22.90 ± 3.29	22.44 ± 3.49	21.89 ± 2.63	22.21 ± 3.14	0.384[a]	0.299[a]
Sex, female/male	19/17	28/13	25/6	53/19	0.052[b]	0.030[b]
headache attack duration	/	10 (8, 24)	12 (8, 24)	12 (8, 24)	0.783[c]	
Headache intensity, VAS	/	8 (7, 9)	9 (8, 10)	8 (7, 10)	0.026[c]	
Monthly migraine days	/	9 (6, 11)	19 (17, 22)	14 (9, 18)	<0.001[c]	
MIDAS score	/	49 (28, 78)	80 (34, 115)	60 (30, 94)	0.079[c]	
HIT-6 score	/	67 (64, 72)	69 (62, 75)	68 (63, 73)	0.457[c]	
GAD-7 score	/	6 (3, 10)	5 (2, 9)	6 (3, 9)	0.576[c]	
PHQ-9 score	/	6 (4, 9)	7 (4, 15)	7 (4, 12)	0.285[c]	
PSQI score	/	7 (5, 10)	5 (4, 9)	7 (4, 10)	0.175[c]	
MMSE score	29 (28, 30)	26 (0, 29)	28 (26, 30)	27 (25, 29)	0.007[c]	0.015[c]
MoCA score	29 (28, 30)	26 (25, 29)	25 (24, 29)	26 (24, 29)	0.009[c]	0.002[c]

Note: Data are presented as mean ± SD, median (Q1, Q3), or female/male. P_1: Compares the available groups among HC, EM, and CM; when HC has no observations, EM is compared with CM. P_2: Compares HC with the combined migraine group (EM + CM); it is left blank when either comparison group has no observations.[a] Welch two-sample *t*-test or Welch one-way ANOVA; [b] Pearson chi-square test or Fisher's exact test; [c] Wilcoxon rank-sum test or Kruskal-Wallis test.

Group differences in regional SDI

After adjustment for age and sex, the migraine group showed lower SDI in the left superior frontal gyrus (SFG_L_7_4; $q < 0.001$) and higher SDI in the right inferior temporal gyrus (ITG_R_7_3; $q = 0.008$) than HCs (Table 2; Figs. 2a–b and 3a).

Table 2
Brain regions showing significant SDI differences between the migraine and HC groups

Atlas ID	Brain region	Adjusted difference, Migraine - HC(95% CI)	*F*(1, 104)	Partial η²	*p*	FDR *q*
BNA_007	SFG_L_7_4	-0.284(-0.381, -0.188)	34.02	0.246	< 0.001	< 0.001
BNA_094	ITG_R_7_3	0.164(0.086, 0.243)	17.26	0.142	< 0.001	0.008

Note: Adjusted differences were estimated using ANCOVA controlling for age and sex and are expressed as Migraine − HC. Positive and negative values indicate higher and lower SDI in the migraine group, respectively. Only FDR-significant regions are shown. CI, confidence interval; FDR, false discovery rate; HC, healthy controls. ITG, inferior temporal gyrus; SFG, superior frontal gyrus; L, left; R, right.

Significant overall group differences among HCs, EM, and CM were observed in SFG_L_7_4 ($q < 0.001$), the left lateral occipital cortex (LOcC_L_2_1; $q = 0.005$), and ITG_R_7_3 ($q = 0.024$). Pairwise comparisons showed lower SFG_L_7_4 SDI in both EM ($q = 0.015$) and CM ($q < 0.001$) than in HCs, as well as lower values in CM than in EM ($q = 0.017$). CM also showed lower LOcC_L_2_1 SDI than EM ($q = 0.002$), whereas EM showed higher ITG_R_7_3 SDI than HCs ($q = 0.015$). No other pairwise differences survived FDR correction (Table 3; Figs. 2c–e and 3b–d).

Table 3
Brain regions showing significant overall and pairwise differences in SDI among the HC, EM, and CM groups

Atlas ID	Brain region	Overall F(2, 103)	Partial η²	Overall *p*	Overall FDR *q*	Significant pairwise comparison(s)	Adjusted difference (95% CI)	Pairwise *p*	Pairwise FDR *q*
BNA_007	SFG_L_7_4	27.26	0.346	< 0.001	< 0.001	EM - HC	-0.201 (-0.300, -0.101)	< 0.001	0.015
						CM - HC	-0.412 (-0.523, -0.301)	< 0.001	< 0.001
						CM - EM	-0.211 (-0.317,-0.106)	< 0.001	0.017
BNA_207	LOcC _L_2_1	11.06	0.177	< 0.001	0.005	CM - EM	-0.218 (-0.310,-0.125)	< 0.001	0.002
BNA_094	ITG_R_7_3	8.82	0.146	< 0.001	0.024	EM - HC	0.177 (0.090, 0.263)	< 0.001	0.015

Note: ANCOVA was adjusted for age and sex. Adjusted differences were calculated as the first-listed group minus the second-listed group. Only FDR-significant results are shown. ANCOVA, analysis of covariance; CI, confidence interval; CM, chronic migraine; EM, episodic migraine; FDR, false discovery rate; HC, healthy controls; ITG, inferior temporal gyrus; LocC, lateral occipital cortex; SFG, superior frontal gyrus; L, left; R, right.

Associations between SDI alterations and clinical measures

SDI in the left lateral occipital cortex (LOcC_L_2_1) was negatively associated with MMD after adjustment for age, sex, and migraine subtype ($\rho = -0.437$, $q = 0.003$) (Fig. 4). A negative association was also observed between SFG_L_7_4 SDI and GAD-7 scores, but it did not survive FDR correction and is shown only for illustrative purposes ($\rho = -0.241$, $q = 0.474$).

Classification performance of SDI

The SVM models based on regional SDI showed the highest classification performance for distinguishing CM from HCs, with an AUC of 0.866 (95% CI: 0.778–0.943). The AUCs were 0.796 (95% CI: 0.688–0.892) for CM versus EM and 0.770 (95% CI: 0.660–0.867) for EM versus HCs (Fig. 5).

PLS-based gene expression and enrichment results

Metascape analysis showed that genes positively associated with the migraine-minus-HC SDI *t*-map were mainly enriched in processes related to chromatin regulation, transcriptional control, gene silencing, RNA metabolism, and inositol phosphate metabolism. In contrast, negatively associated genes were predominantly enriched in mitochondrial energy metabolism, including oxidative phosphorylation and respiratory-chain complex I assembly, as well as ribosome-associated quality control, macroautophagy, membrane organization, cytoskeletal regulation, and calcium-related signaling (Fig. 6). These positive and negative associations reflect opposite spatial relationships with the SDI difference map and should not be interpreted as differential gene upregulation or downregulation.

Discussion

In this study, we applied the structural decoupling index (SDI) — a graph signal processing approach that quantifies how closely functional activity is constrained by the underlying white matter microstructure — to investigate hierarchical structure–function coupling alterations in migraine. Using radial diffusivity (RD)-weighted structural connectivity as the structural scaffold, we

identified a regionally specific and bidirectional pattern of SDI alterations in patients with migraine relative to healthy controls: SDI was reduced in the left superior frontal gyrus (SFG) and increased in the right inferior temporal gyrus (ITG). Three-group analyses further delineated differential involvement across episodic migraine (EM) and chronic migraine (CM), with the left lateral occipital cortex (LOcC) showing significant SDI reduction in CM relative to EM. Importantly, LOcC SDI was negatively associated with monthly migraine days, and regional SDI features demonstrated moderate-to-good discriminative performance, particularly for distinguishing CM from HCs (AUC = 0.866). Transcriptomic enrichment analyses linked the spatial pattern of SDI alterations to genes involved in chromatin regulation and transcriptional control, as well as mitochondrial energy metabolism and calcium-related signaling. Taken together, these results extend prior findings of globally reduced SFC in migraineby demonstrating regionally specific, bidirectional alterations in hierarchical microstructural–functional organization[18].

The bidirectional pattern of SDI alterations — reduced in the prefrontal cortex and increased in the temporal cortex — may reflect a perturbation of the canonical unimodal-to-transmodal gradient along which SFC is organized in the healthy brain[16, 17]. In the general population, primary sensorimotor regions exhibit close coupling between functional activity and microstructural architecture, whereas higher-order association cortices, including the prefrontal cortex, display relative decoupling — a gradient organization thought to enable functional flexibility and support diverse cognitive repertoires[16, 17]. Here, SFC is operationalized through RD-weighted structural connectivity; RD is a diffusion tensor-derived measure sensitive to multiple aspects of white-matter microstructure, although it is not specific to myelination or axonal integrity. Reduced SDI in SFG may therefore reflect a pathological increase in microstructural constraint on prefrontal functional dynamics, potentially limiting the adaptive repertoire of executive and cognitive control processes. Conversely, heightened SDI in ITG may indicate a loss of microstructural guidance in a region normally more closely coupled to white matter architecture, possibly contributing to aberrant sensory processing.

The functional significance of the identified regions aligns with well-documented domains of impairment in migraine. The SFG is a core node of the prefrontal executive control network, subserving cognitive flexibility, working memory, and top-down regulation of pain and emotion. Structural and functional abnormalities in the prefrontal cortex have been consistently reported in migraine and correlate with executive dysfunction[37, 38]. Resting-state functional connectivity studies have further demonstrated disrupted executive network integrity in patients with migraine, with altered fronto-parietal connectivity correlating with cognitive performance[10]. A recent task-based fMRI study demonstrated prefrontal dysregulation of interoceptive and emotional processing in episodic migraine[39]. The reduced SDI in SFG may thus represent a microstructural substrate linking RD-weighted structural–functional decoupling to the cognitive and affective symptoms commonly experienced by patients with migraine.

The ITG is involved in high-level visual processing and multisensory integration — functions characteristically altered in migraine, as evidenced by photophobia, visual discomfort, and multisensory hypersensitivity[40]. The disconnectome model proposed by Silvestro et al. posits that migraine involves a rearrangement of brain connectivity across sensory processing networks, a view broadly consistent with our finding of increased ITG decoupling from the microstructural scaffold[41].

The LOcC finding is particularly noteworthy given its association with monthly migraine days. The significant SDI difference between EM and CM, together with the negative correlation with monthly migraine days, suggests that LOcC microstructural–functional coupling may track disease progression and chronification. The visual cortex has been implicated in migraine pathophysiology through cortical spreading depression and hyperexcitability, and our data provide preliminary evidence that the hierarchical organization of this region is progressively disrupted with increasing attack frequency[42]. Brain microstructural alterations in migraine have also been shown to correlate with pain catastrophizing and disease severity[43]. The progression from episodic to chronic migraine involves alterations in pain network dynamics and, as suggested by longitudinal neuroimaging studies, potential structural connectivity reorganization[4, 5]. Diffusion imaging studies have revealed white matter microstructural alterations in CM relative to EM across distributed cortical pathways, including frontal, visual, and sensorimotor regions[44], and enhanced connectivity within the pain matrix has been associated with increased headache frequency in CM patients[11]. Our finding of progressive LOcC SDI reduction from EM to CM extends this literature by providing preliminary evidence that the structure–function relationship in the visual cortex may become increasingly constrained by microstructural alterations as migraine progresses toward chronicity. The negative association between LOcC SDI and monthly migraine days further highlights the potential clinical relevance of SDI as a quantitative imaging marker of disease burden.

The bidirectional SDI pattern observed in migraine invites comparison with SFC alterations reported in other neurological disorders. Notably, bidirectional alterations in structure–function coupling are not unique to migraine. In Alzheimer's disease, Sun et al. applied the SDI framework in a large multicenter sample and found both increased SDI in temporal, insular, hippocampal, and limbic regions and decreased SDI in the frontal lobe[19], indicating that bidirectional hierarchical disruption may represent a shared feature across neurological conditions, albeit with disorder-specific regional topographies. In major depressive disorder, regional SFC alterations have been linked to neurotransmitter and genetic profiles[45], further supporting the notion that macroscale coupling disruptions reflect underlying molecular variation. Across these conditions, a common theme of disrupted prefrontal regulation and sensory integration emerges, although the specific regional patterns and directionality of coupling alterations appear to differ. Whether these differences reflect true disease-specific signatures or arise from methodological variation in how coupling is quantified remains an open question requiring direct cross-disorder comparisons with standardized analytical frameworks.

The SVM classification results further support the discriminative value of regional SDI. The highest AUC was achieved for CM versus HC classification (0.866), with moderate performance for CM versus EM (0.796) and EM versus HC (0.770). This gradient of classification accuracy — whereby the most clinically distinct groups showed the highest separability — provides preliminary evidence that SDI features capture clinically meaningful dimensions of migraine severity. A recent study investigating SC–FC coupling beyond the cortex in CM further supports the potential of connectivity-based markers for characterizing disease subtypes[46]. Moreover, graph-based connectomics analysis has shown that the topological efficiency of white matter structural networks is disrupted in migraine, with alterations correlating with clinical measures[12]. Together with our findings, these converging lines of evidence indicate that microstructural connectivity markers — particularly those capturing the correspondence between structural and functional architecture — may hold promise for objective disease stratification and monitoring. Compared with the prior connectomics study that reported globally reduced SFC in migraine using conventional correlation-based approaches[18], the SDI framework employed here quantifies region-specific hierarchical dependency rather than pairwise connectivity correspondence, which may account for its improved sensitivity to disease-related alterations.

The spatial correlation between SDI alterations and regional gene expression profiles provides insight into molecular pathways that may underlie disrupted microstructural–functional hierarchy in migraine. Genes positively associated with the SDI difference map were enriched in chromatin regulation, transcriptional control, and RNA-related processes, suggesting that epigenetic and gene regulatory mechanisms contribute to regional vulnerability to SFC disruption. This is broadly compatible with the complex polygenic architecture of migraine revealed by large-scale genome-wide association studies[47] and with evidence that inter-individual variability in regional SFC is under substantial genetic control and associated with neurotransmitter receptor and gene expression profiles[48, 49].

Genes negatively associated with the SDI difference map were enriched in mitochondrial energy metabolism, calcium signaling, and ribosome-associated quality control. This pattern aligns with the growing recognition of mitochondrial dysfunction as a central mechanism in migraine pathophysiology[50–52] and with sex-specific differences in mitochondrial function[53]. The enrichment of oxidative phosphorylation genes in regions showing altered SDI suggests that energy metabolic constraints may contribute to disrupted structure–function coupling by affecting synaptic maintenance and white matter integrity. Calcium channels are established mediators of cortical spreading depression[54], and recent evidence of abnormal glutamatergic and serotonergic connectivity in migraine[55] further implicates neurotransmitter and ion channel dysfunction in the network-level alterations observed here. Altogether, these molecular findings align with the emerging framework connecting macroscale brain network organization to microscale transcriptional and neurotransmitter profiles[45, 49].

Several limitations should be acknowledged. First, the cross-sectional design precludes causal or longitudinal inferences regarding migraine chronification. Second, the sample size was modest, particularly for subgroup analyses, and the findings require replication in larger, independent cohorts. Third, structural graphs were constructed using CSD-based probabilistic tractography, and the observed SDI patterns may depend on the selected graph construction, weighting, and scaling scheme. Fourth, the SVM models were evaluated without external validation, and their generalizability remains uncertain. Fifth, transcriptomic analyses were based on gene-expression data from a small number of healthy postmortem donors and identified spatial associations rather than disease-specific differential expression or causal molecular mechanisms.

Conclusions

In conclusion, migraine was associated with regionally heterogeneous alterations in SDI derived from an RD-weighted structural graph, involving prefrontal, temporal, and occipital regions. Lower LOcC SDI was associated with a greater number of monthly migraine days, suggesting a relationship between regional structure–function organization and clinical disease burden. Regional SDI features also showed preliminary within-sample discriminative performance, although independent validation is required. Exploratory transcriptomic analyses identified spatial associations with gene sets enriched in transcriptional regulation, mitochondrial energy metabolism, and calcium-related signaling. These findings support SDI as a candidate framework for characterizing regional structure–function relationships in migraine but require confirmation using alternative structural weighting schemes, spatially informed transcriptomic analyses, and independent longitudinal cohorts.

List of abbreviations

ANCOVA, analysis of covariance

ANTs, Advanced Normalization Tools

AUC, area under the curve

BH-FDR, Benjamini–Hochberg false discovery rate

BMI, body mass index

BOLD, blood oxygen level dependent

CI, confidence interval

CM, chronic migraine

CONN, functional connectivity toolbox

CSD, constrained spherical deconvolution

dMRI, diffusion magnetic resonance imaging

EM, episodic migraine

FDR, false discovery rate

FSL, FMRIB Software Library

GAD-7, Generalized Anxiety Disorder-7

GRAPPA, generalized autocalibrating partial parallel acquisition

HC, healthy control

HIT-6, Headache Impact Test-6

ICHD-3, International Classification of Headache Disorders, 3rd edition

ITG, inferior temporal gyrus

LOcC, lateral occipital cortex

MIDAS, Migraine Disability Assessment

MMD, monthly migraine days

MMSE, Mini-Mental State Examination

MNI, Montreal Neurological Institute

MoCA, Montreal Cognitive Assessment

MPRAGE, magnetization-prepared rapid gradient echo

MRI, magnetic resonance imaging

PHQ-9, Patient Health Questionnaire-9

PLS, partial least squares

PLS1, first partial least squares component

PSQI, Pittsburgh Sleep Quality Index

RD, radial diffusivity

ROC, receiver operating characteristic

rs-fMRI, resting-state functional magnetic resonance imaging

SDI, structural decoupling index

SFC, structure–function coupling

SFG, superior frontal gyrus

SIFT, spherical-deconvolution informed filtering of tractograms

SPM12, Statistical Parametric Mapping 12

SVM, support vector machine

TE, echo time

TI, inversion time

TR, repetition time

VAS, Visual Analogue Scale

Declarations

Acknowledgments

We deeply appreciate the involvement of all participants in this research.

Ethical considerations

The study protocol was reviewed and approved by the Ethics Committee of Beijing Tiantan Hospital, Capital Medical University (Approval No. KY2022-044).

Consent to participate

Each participant or their guardian provided written informed consent prior to participation.

Consent for publishing

All authors authorize the publication of the article.

Author contributions

The study was conceptualized and designed by ZG, YL, and YGW. ZG conducted the initial data analysis with support from ZHX, YLM, and DQ. ZG, YL, and YGW oversaw data quality control and supervised the study. All authors participated in the collection of clinical and MRI data. ZG drafted the initial manuscript. YL and YGW critically reviewed and revised the manuscript. All authors reviewed and approved the final version of the manuscript.

Declaration of conflicting interests

The authors declared no potential conflicts of interest with respect to the research, authorship, and/or publication of this article.

Funding

This study was supported by the National Key R&D Program of China (grant number 2024YFC2510101); the Joint Funds of the National Natural Science Foundation of China (grant number U24A20683); Beijing Natural Science Foundation (grant number F252058); Shenzhen Medical Research Fund (grant number C2501004).

Data availability statement

The supporting data and materials for this study are available from the corresponding author on reasonable request.

References

1. Gbd 2023 Headache Collaborators (2025) Global, regional, and national burden of headache disorders, 1990–2023: a systematic analysis for the global burden of disease study 2023. Lancet Neurol 24:1005–1015. https://doi.org/10.1016/S1474-4422(25)00402-8
2. Ashina M (2020) Migraine. N Engl J Med 383:1866–1876. https://doi.org/10.1056/NEJMra1915327
3. Raggi A, Leonardi M, Arruda M et al (2024) Hallmarks of primary headache: part 1 - migraine. J Headache Pain 25:189–235. https://doi.org/10.1186/s10194-024-01889-x
4. May A, Schulte LH (2016) Chronic migraine: risk factors, mechanisms and treatment. Nat Rev Neurol 12:455–464. https://doi.org/10.1038/nrneurol.2016.93
5. Filippi M, Messina R (2019) The chronic migraine brain: what have we learned from neuroimaging? Front Neurol 10:1356. https://doi.org/10.3389/fneur.2019.01356
6. Rahimi R, Dolatshahi M, Abbasi-Feijani F et al (2022) Microstructural white matter alterations associated with migraine headaches: a systematic review of diffusion tensor imaging studies. Brain Imaging Behav 16:2375–2401. https://doi.org/10.1007/s11682-022-00690-1
7. Yu D, Yuan K, Qin W et al (2013) Axonal loss of white matter in migraine without aura: a tract-based spatial statistics study. Cephalalgia Int J Headache 33:34–42. https://doi.org/10.1177/0333102412466964
8. Szabó N, Kincses ZT, Párdutz Á et al (2012) White matter microstructural alterations in migraine: a diffusion-weighted MRI study. Pain 153:651–656. https://doi.org/10.1016/j.pain.2011.11.029
9. Li Z, Mei Y, Wang L et al (2025) White matter and cortical gray matter microstructural alterations in migraine: a NODDI and DTI analysis. J Headache Pain 26:115. https://doi.org/10.1186/s10194-025-02059-3
10. Russo A, Tessitore A, Giordano A et al (2012) Executive resting-state network connectivity in migraine without aura. Cephalalgia Int J Headache 32:1041–1048. https://doi.org/10.1177/0333102412457089

11. Lee MJ, Park B-Y, Cho S et al (2019) Increased connectivity of pain matrix in chronic migraine: a resting-state functional MRI study. J Headache Pain 20:29. https://doi.org/10.1186/s10194-019-0986-z
12. Mei Y, Qiu D, Xiong Z et al (2024) Disrupted topologic efficiency of white matter structural connectome in migraine: a graph-based connectomics study. J Headache Pain 25:204. https://doi.org/10.1186/s10194-024-01919-8
13. Huntenburg JM, Bazin P-L, Margulies DS (2018) Large-scale gradients in human cortical organization. Trends Cogn Sci 22:21–31. https://doi.org/10.1016/j.tics.2017.11.002
14. Park H-J, Friston K (2013) Structural and functional brain networks: from connections to cognition. Science 342:1238411. https://doi.org/10.1126/science.1238411
15. Suárez LE, Markello RD, Betzel RF, Misic B (2020) Linking structure and function in macroscale brain networks. Trends Cogn Sci 24:302–315. https://doi.org/10.1016/j.tics.2020.01.008
16. Preti MG, Van De Ville D (2019) Decoupling of brain function from structure reveals regional behavioral specialization in humans. Nat Commun 10:4747. https://doi.org/10.1038/s41467-019-12765-7
17. Fotiadis P, Parkes L, Davis KA et al (2024) Structure–function coupling in macroscale human brain networks. Nat Rev Neurosci 25:688–704. https://doi.org/10.1038/s41583-024-00846-6
18. Li K, Liu L, Yin Q et al (2017) Abnormal rich club organization and impaired correlation between structural and functional connectivity in migraine sufferers. Brain Imaging Behav 11:526–540. https://doi.org/10.1007/s11682-016-9533-6
19. Sun Y, Wang P, Zhao K et al (2024) Structure–function coupling reveals the brain hierarchical structure dysfunction in alzheimer's disease: a multicenter study. Alzheimers Dement 20:6305–6315. https://doi.org/10.1002/alz.14123
20. (2018) Headache classification committee of the international headache society (IHS) the international classification of headache disorders, 3rd edition. Cephalalgia Int J Headache 38:1–211. https://doi.org/10.1177/0333102417738202
21. Price DD, McGrath PA, Rafii A, Buckingham B (1983) The validation of visual analogue scales as ratio scale measures for chronic and experimental pain. Pain 17:45–56. https://doi.org/10.1016/0304-3959(83)90126-4
22. Stewart WF, Lipton RB, Dowson AJ, Sawyer J (2001) Development and testing of the migraine disability assessment (MIDAS) questionnaire to assess headache-related disability. Neurology 56:S21–28. https://doi.org/10.1212/wnl.56.suppl_1.s20
23. Kosinski M, Bayliss MS, Bjorner JB et al (2003) A six-item short-form survey for measuring headache impact: the HIT-6. Qual Life Res Int J Qual Life Asp Treat Care Rehabil 12:963–974. https://doi.org/10.1023/a:1026119331193
24. Spitzer RL, Kroenke K, Williams JBW, Löwe B (2006) A brief measure for assessing generalized anxiety disorder: the GAD-7. Arch Intern Med 166:1092–1097. https://doi.org/10.1001/archinte.166.10.1092
25. Kroenke K, Spitzer RL, Williams JB (2001) The PHQ-9: validity of a brief depression severity measure. J Gen Intern Med 16:606–613. https://doi.org/10.1046/j.1525-1497.2001.016009606.x
26. Buysse DJ, Reynolds CF, Monk TH et al (1989) The pittsburgh sleep quality index: a new instrument for psychiatric practice and research. Psychiatry Res 28:193–213. https://doi.org/10.1016/0165-1781(89)90047-4
27. Folstein MF, Folstein SE, McHugh PR (1975) Mini-mental state. A practical method for grading the cognitive state of patients for the clinician. J Psychiatr Res 12:189–198. https://doi.org/10.1016/0022-3956(75)90026-6
28. Nasreddine ZS, Phillips NA, Bédirian V et al (2005) The Montreal cognitive assessment, MoCA: a brief screening tool for mild cognitive impairment. J Am Geriatr Soc 53:695–699. https://doi.org/10.1111/j.1532-5415.2005.53221.x
29. Tournier J-D, Smith R, Raffelt D et al (2019) MRtrix3: a fast, flexible and open software framework for medical image processing and visualisation. NeuroImage 202:116137. https://doi.org/10.1016/j.neuroimage.2019.116137
30. Jenkinson M, Beckmann CF, Behrens TEJ et al (2012) Fsl NeuroImage 62:782–790. https://doi.org/10.1016/j.neuroimage.2011.09.015
31. Avants BB, Tustison NJ, Song G et al (2011) A reproducible evaluation of ANTs similarity metric performance in brain image registration. NeuroImage 54:2033–2044. https://doi.org/10.1016/j.neuroimage.2010.09.025
32. Fischl B (2012) FreeSurfer NeuroImage 62:774–781. https://doi.org/10.1016/j.neuroimage.2012.01.021
33. Bortolin K, Delavari F, Preti MG et al (2022) Neural substrates of psychosis revealed by altered dependencies between brain activity and white-matter architecture in individuals with 22q11 deletion syndrome. NeuroImage Clin 35:103075. https://doi.org/10.1016/j.nicl.2022.103075

34. Hawrylycz MJ, Lein ES, Guillozet-Bongaarts AL et al (2012) An anatomically comprehensive atlas of the adult human brain transcriptome. Nature 489:391–399. https://doi.org/10.1038/nature11405
35. Markello RD, Arnatkeviciute A, Poline J-B et al (2021) Standardizing workflows in imaging transcriptomics with the abagen toolbox. eLife 10:e72129. https://doi.org/10.7554/eLife.72129
36. Zhou Y, Zhou B, Pache L et al (2019) Metascape provides a biologist-oriented resource for the analysis of systems-level datasets. Nat Commun 10:1523. https://doi.org/10.1038/s41467-019-09234-6
37. Schmitz N, Arkink EB, Mulder M et al (2008) Frontal lobe structure and executive function in migraine patients. Neurosci Lett 440:92–96. https://doi.org/10.1016/j.neulet.2008.05.033
38. Kaiser Pinotti L, Castro A da, de Oliveira Garcia S GH, et al (2023) Executive functions in migraine patients: a systematic review with meta-analysis. Cognit Neuropsychiatry 28:52–66. https://doi.org/10.1080/13546805.2022.2149390
39. Li Y, Liu R, Lin C et al (2026) Prefrontal dysregulation of interoceptive and emotional processing in episodic migraine: a task-based fMRI study. J Headache Pain 27:111. https://doi.org/10.1186/s10194-026-02329-8
40. Schwedt TJ (2013) Multisensory integration in migraine. Curr Opin Neurol 26:248–253. https://doi.org/10.1097/WCO.0b013e328360edb1
41. Silvestro M, Tessitore A, Caiazzo G et al (2021) Disconnectome of the migraine brain: a connectopathy model. J Headache Pain 22:102. https://doi.org/10.1186/s10194-021-01315-6
42. Yu Y, Zhao H, Dai L et al (2021) Headache frequency associates with brain microstructure changes in patients with migraine without aura. Brain Imaging Behav 15:61–67. https://doi.org/10.1007/s11682-019-00232-2
43. Hubbard CS, Khan SA, Keaser ML et al (2014) Altered brain structure and function correlate with disease severity and pain catastrophizing in migraine patients. eNeuro 1. https://doi.org/10.1523/ENEURO.0006-14.2014. e20.14
44. Planchuelo-Gómez Á, García-Azorín D, Guerrero ÁL et al (2020) Structural connectivity alterations in chronic and episodic migraine: a diffusion magnetic resonance imaging connectomics study. Cephalalgia Int J Headache 40:367–383. https://doi.org/10.1177/0333102419885392
45. Chu T, Si X, Xie H et al (2025) Regional structural-functional connectivity coupling in major depressive disorder is associated with neurotransmitter and genetic profiles. Biol Psychiatry 97:290–301. https://doi.org/10.1016/j.biopsych.2024.08.022
46. Li Y, Hu Y, Dai C et al (2026) Abnormal structural connectivity-functional connectivity coupling beyond the cortex in patients with chronic migraine. J Headache Pain 27:180. https://doi.org/10.1186/s10194-026-02397-w
47. Sutherland HG, Jenkins B, Griffiths LR (2024) Genetics of migraine: complexity, implications, and potential clinical applications. Lancet Neurol 23:429–446. https://doi.org/10.1016/S1474-4422(24)00026-7
48. Gu Z, Jamison KW, Sabuncu MR, Kuceyeski A (2021) Heritability and interindividual variability of regional structure-function coupling. Nat Commun 12:4894. https://doi.org/10.1038/s41467-021-25184-4
49. Jiang L, Genon S, Ye J et al (2025) Gene transcription, neurotransmitter, and neurocognition signatures of brain structural-functional coupling variability. Nat Commun 16:7623. https://doi.org/10.1038/s41467-025-63000-5
50. Gross EC, Lisicki M, Fischer D et al (2019) The metabolic face of migraine - from pathophysiology to treatment. Nat Rev Neurol 15:627–643. https://doi.org/10.1038/s41582-019-0255-4
51. Savran OY, Tuncer M (2025) Possible role of novel mitochondrial subsets in migraine. Life 15:1273. https://doi.org/10.3390/life15081273
52. Sun W-X, Chen T-Y, Song M-M et al (2025) Energy metabolism disorders in migraine: triggers, pathways, and therapeutic repurposing. Front Neurol 16:1561000. https://doi.org/10.3389/fneur.2025.1561000
53. Fila M, Przyslo L, Derwich M et al (2025) Sexual dimorphism in migraine. Focus on mitochondria. Curr Pain Headache Rep 29:11. https://doi.org/10.1007/s11916-024-01317-4
54. Pietrobon D, Moskowitz MA (2013) Pathophysiology of migraine. Annu Rev Physiol 75:365–391. https://doi.org/10.1146/annurev-physiol-030212-183717
55. Puledda F, Dipasquale O, Gooddy BJM et al (2023) Abnormal glutamatergic and serotonergic connectivity in visual snow syndrome and migraine with aura. Ann Neurol 94:873–884. https://doi.org/10.1002/ana.26745

Figures

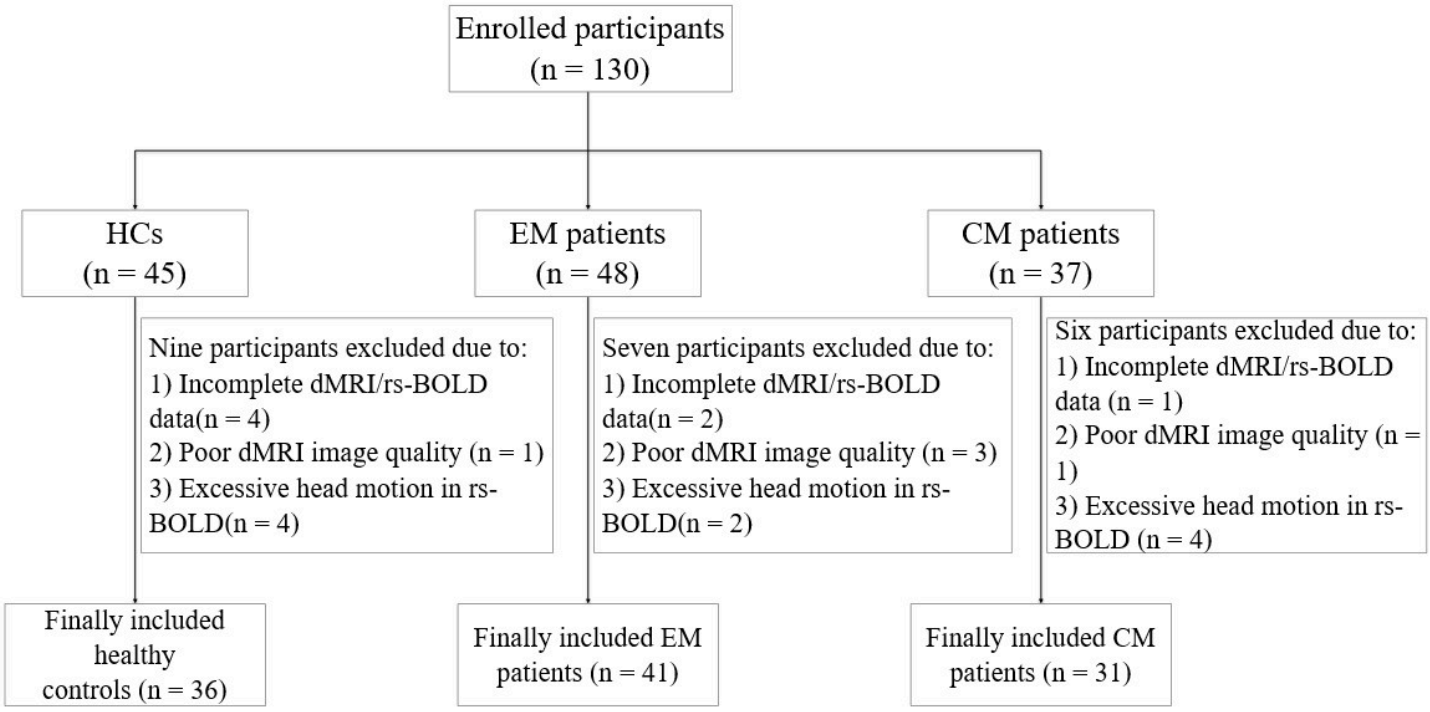

Figure 1

Participant recruitment flowchart.

Note: HC, healthy control; EM, episodic migraine; CM, chronic migraine;

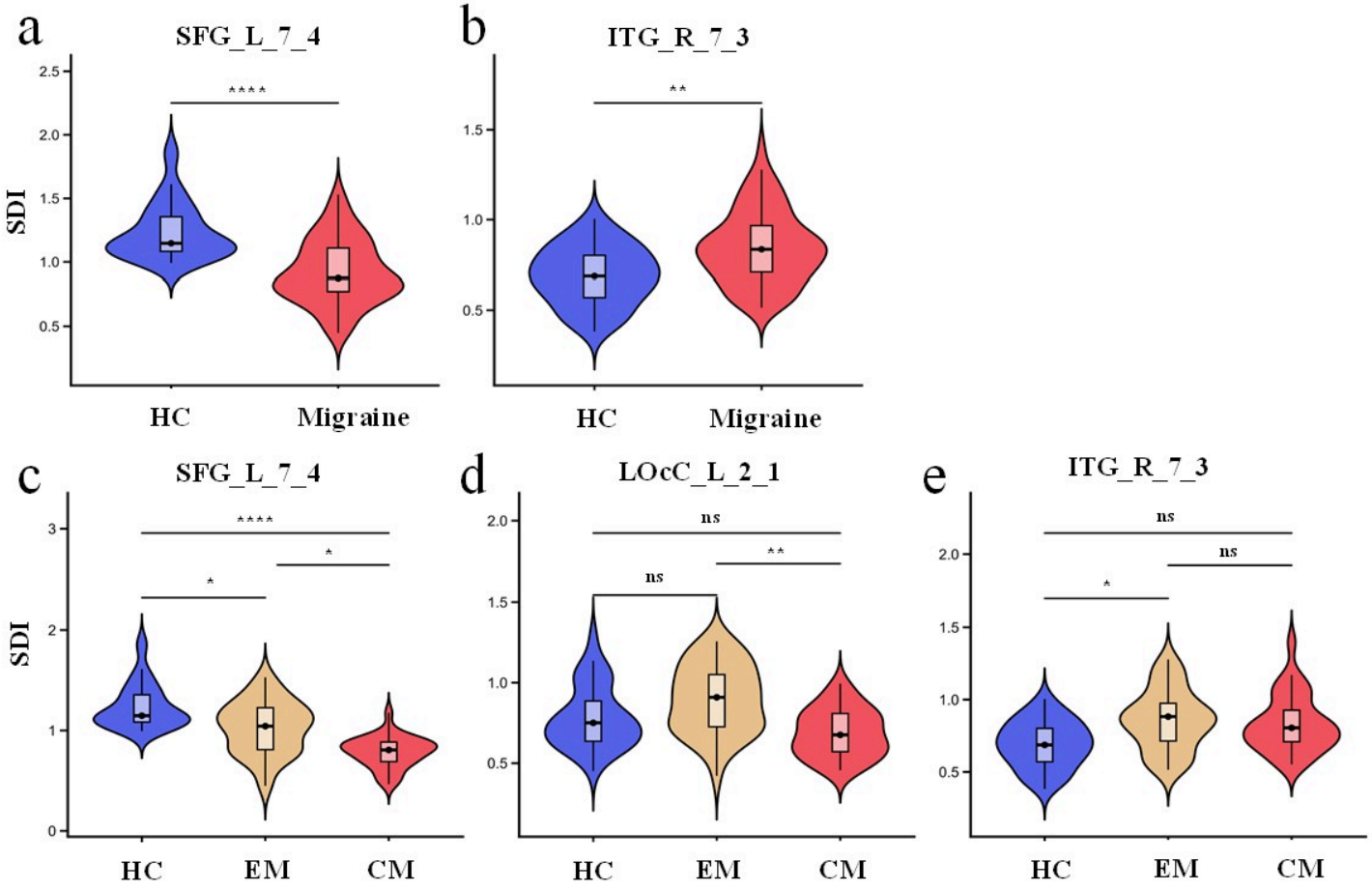

Figure 2

Violin plots showing regional SDI values across groups

Note: (a, b) Comparisons between HCs and the migraine group in SFG_L_7_4 and ITG_R_7_3, respectively. (c–e) Comparisons among HCs, EM patients, and CM patients in SFG_L_7_4, LOcC_L_2_1, and ITG_R_7_3, respectively. ns, $q > 0.05$; *, $q \leq 0.05$; **, $q \leq 0.01$; ***, $q \leq 0.001$; and ****, $q \leq 0.0001$. SDI, structural decoupling index; HC, healthy control; EM, episodic migraine; CM, chronic migraine; SFG, superior frontal gyrus; ITG, inferior temporal gyrus; LOcC, lateral occipital cortex; L, left; R, right; ns, not significant.

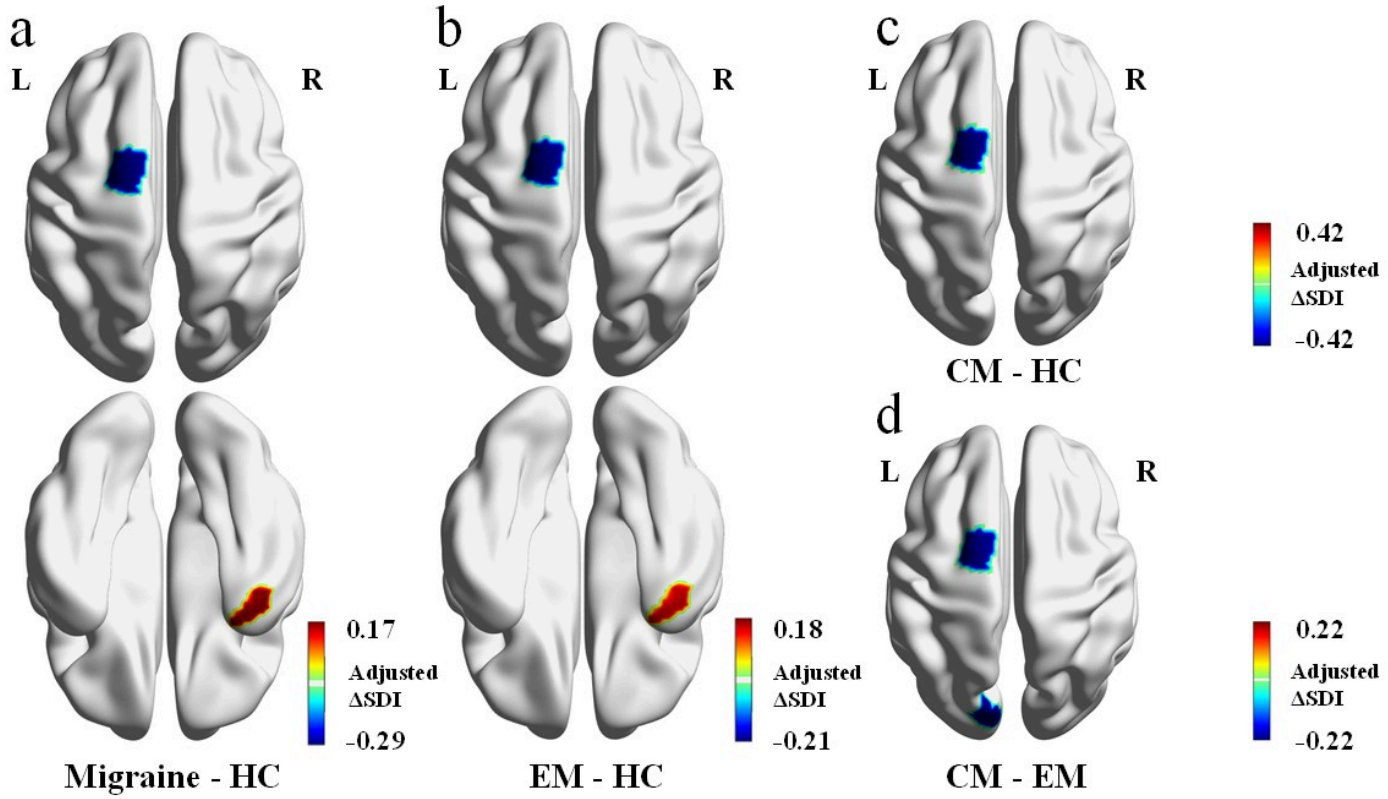

Figure 3

Regional differences in SDI between groups.

Note: (a) Significant differences between the migraine and HC groups; (b) significant differences between the EM and HC groups; (c) significant differences between the CM and HC groups; and (d) significant differences between the CM and EM groups. Colors represent the adjusted between-group differences in SDI, calculated as the first-listed group minus the second-listed group. Warmer and cooler colors indicate positive and negative adjusted differences, respectively. All displayed results survived FDR correction ($q < 0.05$). SDI, structural decoupling index; HC, healthy controls; EM, episodic migraine; CM, chronic migraine; FDR, false discovery rate.

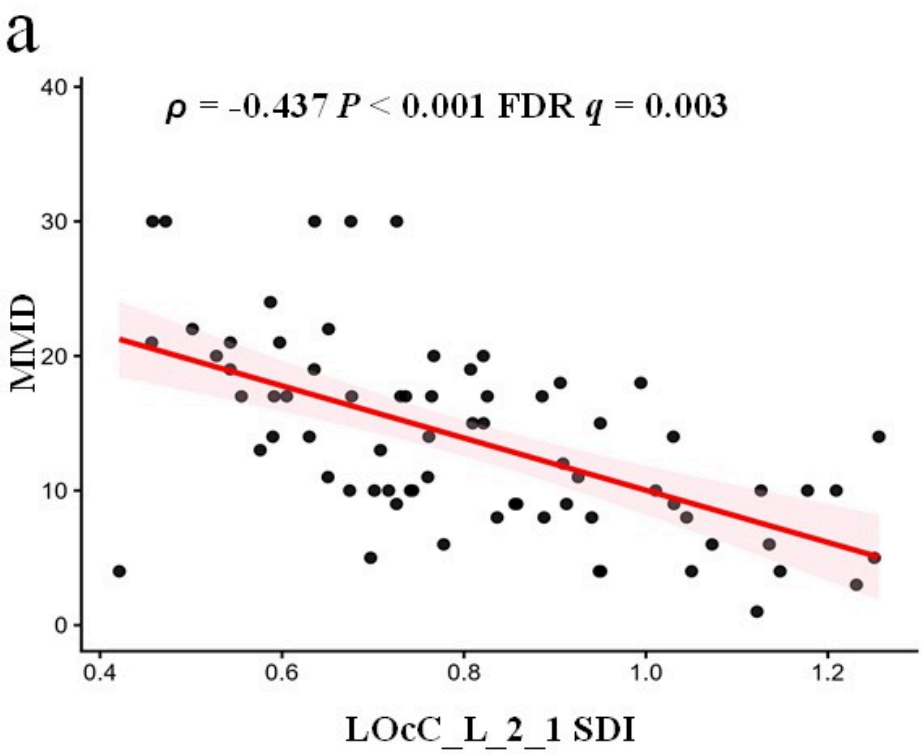

Figure 4

Associations between regional SDI values and clinical measures in patients with migraine.

Note: Association between SDI in LOcC_L_2_1 and MMD. The red lines represent the fitted linear regression lines, and the shaded areas indicate the 95% confidence intervals. SDI, structural decoupling index; MMD, monthly migraine days; LOcC, lateral occipital cortex.

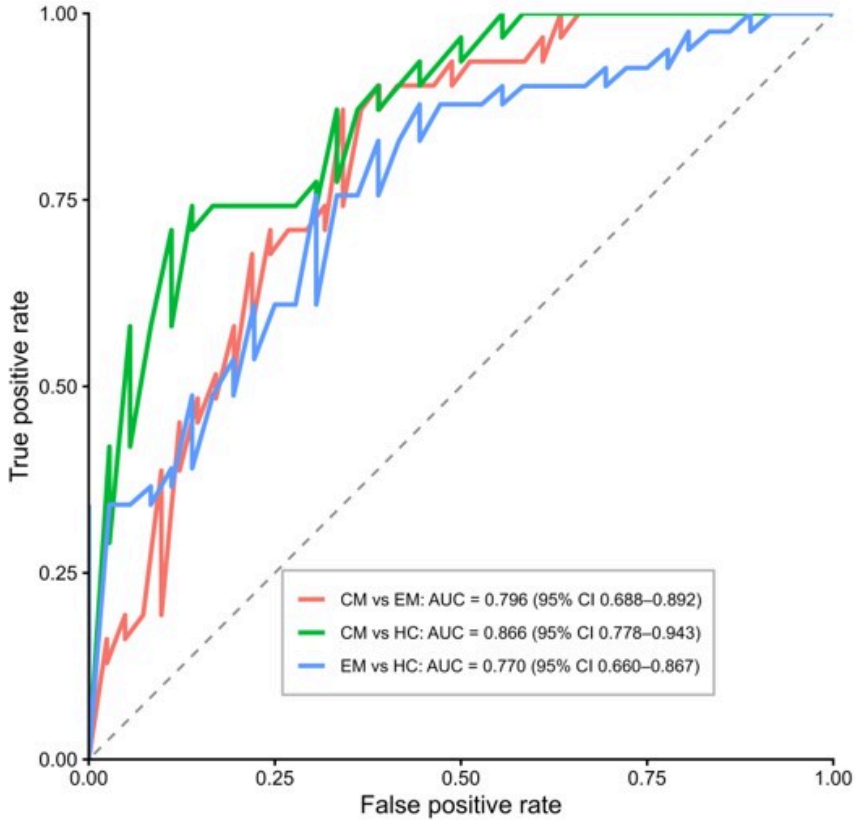

Figure 5

ROC curves for group classification based on regional SDI.

Note: The dashed diagonal line indicates chance-level classification performance. ROC, receiver operating characteristic; AUC, area under the curve; CI, confidence interval; SDI, structural decoupling index; HC, healthy control; EM, episodic migraine; CM, chronic migraine.

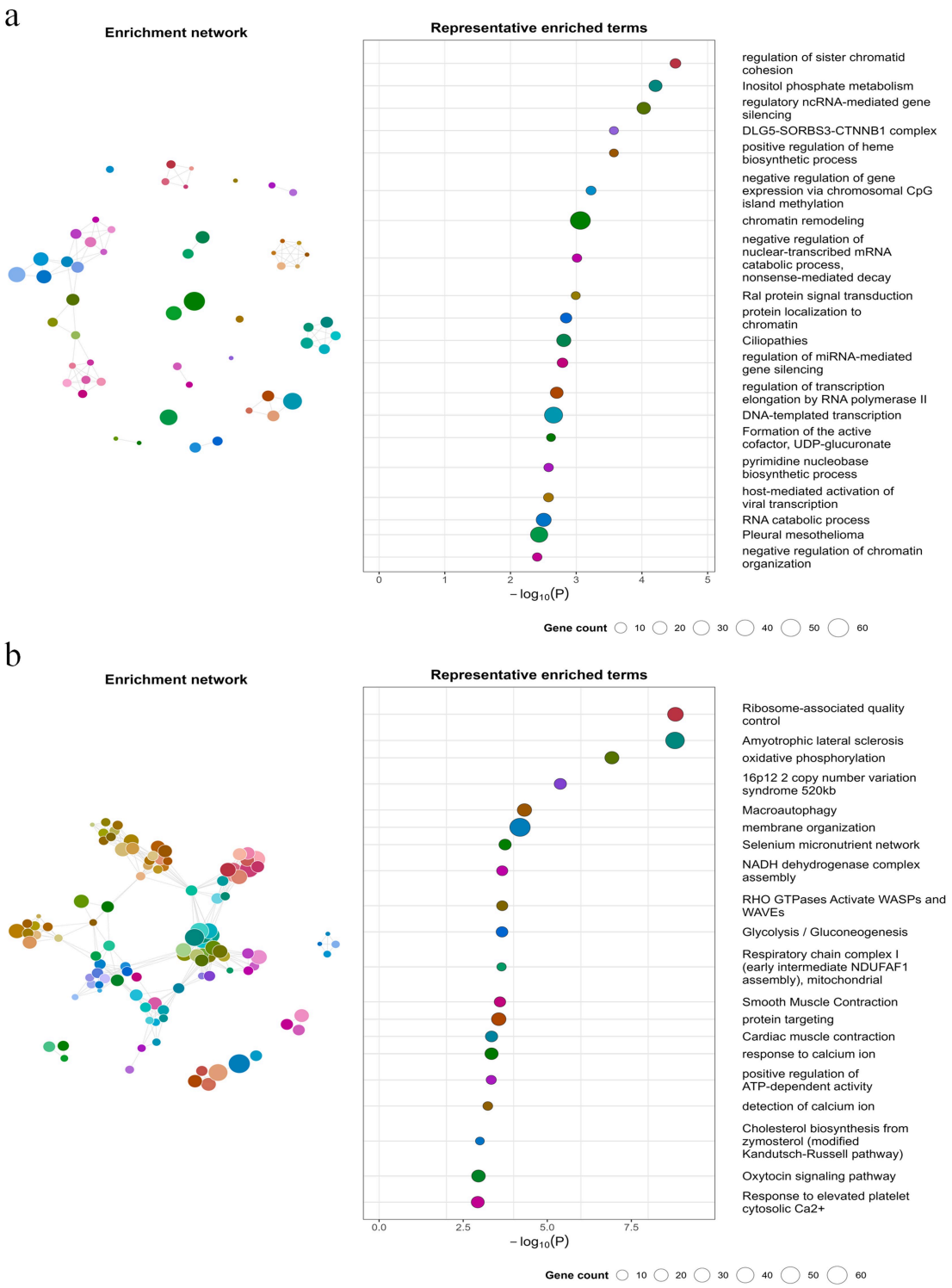

Figure 6

Functional enrichment of genes associated with the spatial pattern of SDI alterations.

(a) Enrichment results for genes positively associated with the migraine-minus-HC SDI t-map. (b) Enrichment results for genes negatively associated with the migraine-minus-HC SDI t-map. In each panel, the enrichment network shows relationships among enriched terms, whereas the bubble plot presents representative enriched terms. Node and bubble sizes indicate gene counts, colors represent enriched-term clusters, and the x-axis indicates -$\log_{10}$ (P). SDI, structural decoupling index; HC, healthy control.